Journal of Applied Polymer Science

Stress memory of a thermoset shape memory polymer

Anqi Wang,[1] Guoqiang Li[1,2]
[1]Department of Mechanical & Industrial Engineering, Louisiana State University, Baton Rouge, Louisiana 70803
[2]Department of Mechanical Engineering, Southern University, Baton Rouge, Louisiana 70813
Correspondence to: G. Li (E-mail: lguoqi1@lsu.edu)

ABSTRACT: The performance of stress recovery and shape recovery are equally important for high performance shape memory polymers (SMPs) in emerging applications. However, unlike shape recovery, stress recovery does not always follow a monotonic behavior, i.e., "stress plateau," "stress overshoot," and "stress undershoot" can be observed. In order to reveal the complicated stress memorization and recovery behavior, this study employs a phenomenological model which considers the recovery stress as the sum of residual programming stress, memorized stress, thermal stress, and relaxed stress for amorphous crosslinked SMPs. This model is demonstrated by a stress recovery experiment in which a polystyrene based SMP was programmed at two prestrain levels above the glass transition temperature, i.e., 20% (neo-Hookean hyperelastic region) and 50% (strain-hardening region), and two fixation temperatures, i.e., 20°C (below T_g) and 45°C (within the T_g region), respectively. In addition, a clear distinction between the memorized stress and recovery stress is presented. © 2015 Wiley Periodicals, Inc. J. Appl. Polym. Sci. **2015**, *132*, 42112.

KEYWORDS: mechanical properties; stimuli-sensitive polymers; thermosets

Received 24 September 2014; accepted 9 February 2015
DOI: 10.1002/app.42112

INTRODUCTION

Thermal-induced shape memory polymers (SMPs) have attracted increasing attention in recent years due to their various applications, such as sensors, actuators, and biomedical devices.[1–7] While numerous studies have been conducted on both strain memory and stress memory, the focus is on strain memory. The strain memory effect is the shape memory effect, i.e., a material can retain its deformed temporary shape either after cooling below a trigger temperature, such as the glass transition temperature (T_g), or without cooling if cold compression or stretch programming is conducted,[8–11] and then recover its initial permanent shape upon heating above the trigger temperature. For amorphous covalently crosslinked SMPs, this effect is driven by the entropic behaviors of the polymer networks. In particular, below T_g, movements of the polymer segments are restricted. When subsequently heated above T_g, the rotation around the segment bonds becomes increasingly unimpeded, and most macromolecules will form compact random coil conformations due to entropic favor, resulting in a recovery to the initial permanent shape.[12,13]

However, in some biomedical and engineering applications, stress recovery usually plays a more important role. For example, when SMP wires are used as sutures, the recovery force by the wire decides the ability to close the wound.[14] In biomedical applications, when SMPs are used as microactuators for treating stroke, the recovery force is crucial since it must be in a certain range without causing collateral damage and maintaining the functionality of the device.[15] A recent application is to use the recovery force to close wide-opened cracks in engineering structures, according to a biomimetic close-then-heal (CTH) scheme.[16,17] The self-healing is further divided into two subcategories, those based on SMP matrix and those based on dispersed SMP fibers. In the subcategory of using SMP based matrix, the crack closure is through constrained volume expansion of the compression programmed SMP matrix[18–20]; alternatively, in the subcategory of using dispersed SMP fibers, the crack closure is through constrained shrinkage of stretch programmed SMP fibers.[21–23] As discussed by these previous studies, stress recovery is more important than strain recovery for suturing or closing cracks. The reason is that in these applications, the constraint by the surrounding materials and structure boundaries must be overcome before the opening can be closed. Obviously, even if the strain recovery ratio is 100%, the opening or crack cannot be closed if the recovery stress is not sufficient to overcome these constraints.

Therefore, it is desired to understand the stress recovery and memory effect of SMPs. In general, the stress memory response for SMPs is uniquely studied via thermomechanical cycles. Typically, one thermomechanical cycle involves deformation at a temperature either above or below a trigger temperature, such

T_g (prestraining), followed by cooling (or without cooling for cold-programming) while maintaining the stress or strain constant, and then load removal, which completes programming, and reheating to trigger specimen returning to its initial shape or stress, which completes the recovery. In an unconstrained shape-recovery experiment (free strain recovery), the ends of the specimen are free, and the strain is monitored to study the strain memory effect. In a constrained recovery experiment (stress recovery), the ends of the specimen are fixed, and the recovery force is monitored to study the stress memory effect. Normally, in a strain recovery experiment, the recovery strain is gradually approaching a plateau as the temperature is increasing above the trigger temperature; while in a stress recovery experiment, the situation is more complicated. In some cases the recovery stress follows a similar pattern to strain recovery, i.e., gradually approaches to a plateau.[24,25] In some other cases, however, "stress undershoot" and "stress overshoot" are observed. For example, the recovery stress of a stretching programmed SMP can even decrease during initial heating and then increase.[26–29] In addition, the recovery stress of compression programmed SMP can experience an overshoot, i.e., a stress peak appears during the recovery process.[16,30,31] Similar effects are also observed in stretch,[32,33] shear,[34] and bending cases.[35,36] In other words, mechanisms other than shape memory itself may be involved in the stress recovery process.

It is necessary to understand the stress evolution of SMPs before putting them into service. Most of the current models that describe the stress recovery behaviors of SMPs can be classified into two categories. The first type is considered the phase transition approach. By introducing active phase and frozen phase, the stress behavior of the glassy, leathery, and rubbery state of SMPs as temperature varies can be modeled. For example, Liu *et al.*,[27] studied uniaxial deformation and stress recovery of an amorphous thermoset polymer and developed micromechanics constitutive models based on internal energy and conformational entropy. Xu and Li used a similar strategy and modeled the thermomechanical behavior of SMP based syntactic foam.[37] Wang *et al.*,[38] considered the frozen retardant time based on Liu's model. Chen and Lagoudas,[39,40] developed a generalized constitutive theory on large deformation and linearized it for small deformation which could predict the stress recovery results reported by Liu *et al.*[27] Qi *et al.*,[30] considered the stress response of a thermoset SMP by the rule-of-mixtures approach from three distinct phases, the rubbery phase, the initial glassy phase present in the undeformed configuration, and the frozen glassy phase newly formed during cooling. The phase transition approach can be applied to a wide variety of SMPs with several transition mechanisms. However, it is considered phenomenological for amorphous SMPs and fails to predict the "stress overshoot" during recovery. The second type of stress recovery model is the thermoviscoelastic approach, which attributes the stress recovery to the change of viscosity, or relaxation time of the polymer. Those models include, for example, early model for polyurethane SMPs by Tobushi *et al.*,[26,41] finite strain 3D thermoviscoelastic model by Diani *et al*,[42] model incorporating structural and stress relaxation for amorphous SMPs by Nguyen *et al.*,[43,44] model by Li and Xu,[8] and Xu and Li,[45] on cold-compression programmed SMP and SMP based syntactic foam, model coupling the nonequilibrium structural relaxation and temperature dependent viscoelasticity to describe the "stress overshoot" behavior by Castro *et al.*,[31] multibranch model by Westbrook *et al.*,[46] model by Xiao *et al.*[47] To describe the recovery stress of SMP programmed below T_g, model implemented in Abaqus to predict the stress recovery of acrylate network SMP by Arrieta *et al.*,[48] and model composed of revised standard linear solid (SLS) element and thermal expansion element for epoxy based SMP by Chen *et al.*[49] The thermoviscoelastic approach can more accurately capture the stress recovery evolution, while the limitation is that it requires a large number of material parameters and calibration work. To reduce the curve-fitting effort and make the model more general for SMPs with various morphologies, Shojaei and Li,[50] developed a statistic mechanics based model, which considers functional and mechanical damage effects during themromechanical cycle and during service.

For engineering applications, a simple model with minimum material parameters to predict the recovery stress evolution of thermal-induced SMP would be helpful. In this work, we experimentally studied the stress evolution during the recovery of a covalently crosslinked thermosetting styrene-based SMP, and then proposed a simple 1D phenomenological model based on phase transition, incorporating both thermal effect and stress relaxation effect, to describe the complex stress recovery behaviors, such as "stress plateau," "stress overshoot," and "stress undershoot." In addition, via this model, a clear distinction between memorized stress and recovery stress was revealed.

EXPERIMENTAL

Materials and Specimen Preparation

The styrene-based shape memory polymer was in-house synthesized according to established procedures.[51] Briefly, vinyl-benzene, vinyl neodecanoate, divinyl-benzene, and benzoyl peroxide (as radical initiator) were mixed according to a precalculated ratio followed by vigorous stirring until a clear viscous solution was obtained. Then, the solution was cast into a rigid mold covered with Teflon sheets, which was then sealed and placed in an oven for curing, at 65°C for 10 h, 75°C for 5 h, and 85°C for 1 h. In general, this styrene-based thermoset SMP was an amorphous covalently crosslinked polymer system (class I in the Ref. [2]) with a glass transition zone from 43 to 78°C, which was confirmed by DSC measurements. In addition, neither decomposition nor additional curing was observed during the temperature scan of DSC, which indicates the samples were fully cured. Specimens were cut from the same batch of cured resin by water jetting to reduce interference of material properties by all means. At least three specimens were used for each type of experiment, but only one result from one set of tests is shown for clarity purposes.

Isothermal Uniaxial Compression Experiments

A series of isothermal uniaxial compression tests covering a wide range of temperatures (25°C, 35°C, 45°C, 55°C, 65°C, 75°C, and 85°C) from glassy state to rubbery state were performed with MTS QTEST/150 testing system to determine the evolution of modulus with temperature, which would be used

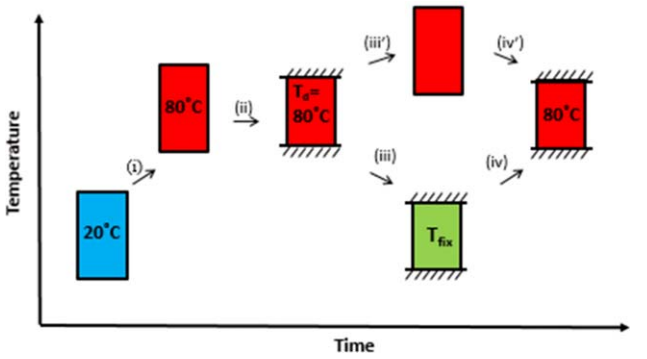

Figure 1. A schematic of the thermomechanical history for a typical stress memory cycle showing programming and recovery. [Color figure can be viewed in the online issue, which is available at wileyonlinelibrary.com.]

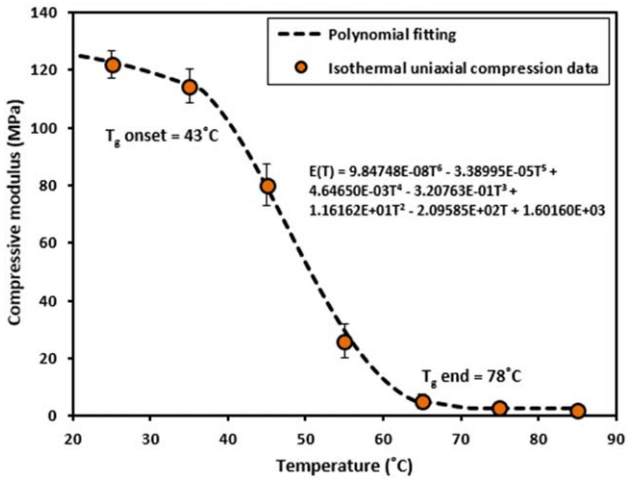

Figure 2. Result of isothermal uniaxial compression tests on SMP samples at different temperatures (25°C, 35°C, 45°C, 55°C, 65°C, 75°C, and 85°C, respectively). The dotted line denotes a continuous plot of compressive modulus as a function of temperature through polynomial curve fitting. [Color figure can be viewed in the online issue, which is available at wileyonlinelibrary.com.]

to calculate the thermal stress accumulation in the recovery stress formulation section. Before compression, the specimen was placed into a temperature-controlled thermal chamber for 30 min to ensure a uniform temperature distribution. Then the specimen was compressed with a crosshead speed of 1.3 mm/min. The dimension of the specimen was: 19.5 × 19.5 × 39.5 mm^3. In general, the detailed experimental procedure is similar to that described in previous studies[46,52] and the calibration of the stress–strain data due to machine compliance followed the method described in the literature.[53] The modulus of the specimen is determined by drawing a tangent to the initial linear portion of the stress strain curve and selecting any point on this straight line portion, and dividing its compressive stress by its corresponding strain, according to ASTM D695 standard.

Programming and Stress Memory Experiments

As shown in Figure 1, thermomechanical cycling tests were carried out in the following steps: (i) Specimen that initially at room temperature (20°C) was placed into an oven of 80°C for 60 min to achieve a uniform temperature distribution in the specimen. (ii) At 80°C, the specimen was uniaxially compressed at a constant deformation rate of 1.3 mm/min to a prescribed prestrain level (20% and 50%, respectively). (iii) The prestrain level was maintained and the specimen was cooled to an assigned fixation temperature T_{fix} (20 and 45°C, respectively) with sufficient dwelling time (more than 10 h). (iv) Without unloading, the specimen was heated up to 80°C again, and the stress response was recorded while maintaining the prestrain level. In general, there are two type of experiments to investigate the stress recovery behavior, namely stress recovery at the predeformation strain level (no unloading at low temperature) and stress recovery at a strain level fixed at a low temperature (unloading at low temperature), as discussed by Liu *et al.*[27] The stress memory experiment was chosen to recover at the predeformation strain level because the residual programming stress would not be zero in general in real world applications and the results will be in a more general sense, whereas stress recovery at a strain level fixed at a low temperature is a special case in which the residual programming stress is simply zero. During the heating and cooling process, a thermal couple was attached to the specimen in order to capture the instantaneous temperature variance of the specimen.

In Figure 1, step (i), (ii), (iii) and (iv) are the actual steps that performed in the stress memory experiment, while step (iii′) and (iv′) are the illustrative fictive steps that show a path equivalent to the actual experimental steps, which are used to verify the simulation results and will be discussed later. (Step (iii′): At 80°C, the specimen was allowed to expand freely without any constraints. step (iv′): Maintaining the temperature at 80°C, the specimen was compressed to the same strain level as that in step (iv) by an equivalent load).

RESULTS AND DISCUSSION

Isothermal Uniaxial Compression Results

The result of the isothermal uniaxial compression is presented in Figure 2. It shows the influence of temperature on mechanical properties of the styrene-based SMP. When the temperature is increased, the modulus decreases due to increasing in mobility of the polymer networks. At room temperature, the specimen has a glassy modulus about 120 MPa, whereas at above 80°C, the specimen has a rubbery modulus of 1–2 MPa. A continuous plot of modulus as a function of temperature through polynomial curve fitting is also shown. From Figure 2, the glass transition zone, which shows a fast decrease in modulus, can be clearly identified.

The behavior of the styrene-based SMP under compression at 80°C (the programming temperature) with a deformation rate of 1.3 mm/min is shown in Figure 3. An incompressible neo-Hookean type of behavior for 1D uniaxial compression with the relation of $\sigma = G[(1+\varepsilon) - (1+\varepsilon)^{-2}]$,[54,55] where G is approximately taken as one third of the Young's modulus due to incompressibility, is also plotted for comparison purpose. It is seen that at a strain of 20%, the modulus is about 1.1 MPa and the incompressible neo-Hookean model is able to capture the quasi-linear behavior quite well; whereas at a strain of 50%, the modulus increases to 1.4 MPa, and the material does not follow

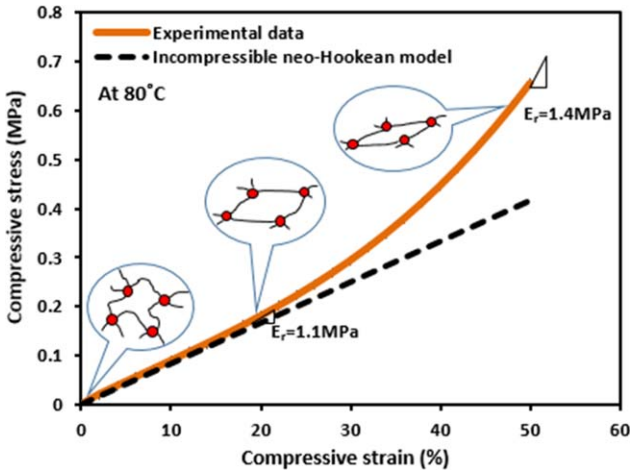

Figure 3. Experimental results for the styrene-based SMP compression programmed at 80°C as compared to the incompressible Neo-Hookean type of behavior. (Note that all the data are presented in the form of engineering stress and engineering strain and the schematic representation of the crosslink net points during deformation is a phenomenological sketch for understanding the stress memory mechanism). [Color figure can be viewed in the online issue, which is available at wileyonlinelibrary.com.]

the incompressible neo-Hookean behavior. In addition, a notable strain hardening effect presents, i.e., the modulus increases with increasing strain. It is believed that initially the crosslinked net-points can move relative to each other when a stress is applied. However, at a certain point the movements of net-points are dramatically restricted due to the limiting stretch of the polymer network,[46,56] which is about 0.8 here (20% strain). As the strain is further increased, the polymer network becomes more difficult to deform, which results in strain hardening. As discussed in the introduction section, the stress memory of SMP relies on the shape memory mechanism under a constraint condition. Since the crosslinked net-points are primarily responsible for the permanent shape, they are also crucial for the stress

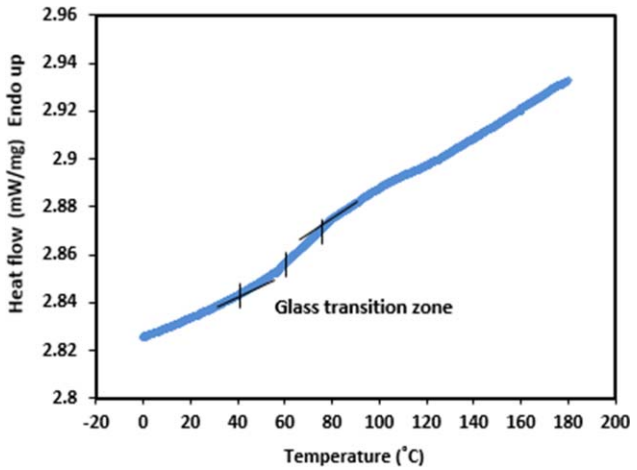

Figure 4. DSC plot of the styrene-based shape memory polymer with a heating rate of 10°C/min, according to ASTM E1356. The sample weight was about 8 mg and the second heating cycle was used to determine the T_g. [Color figure can be viewed in the online issue, which is available at wileyonlinelibrary.com.]

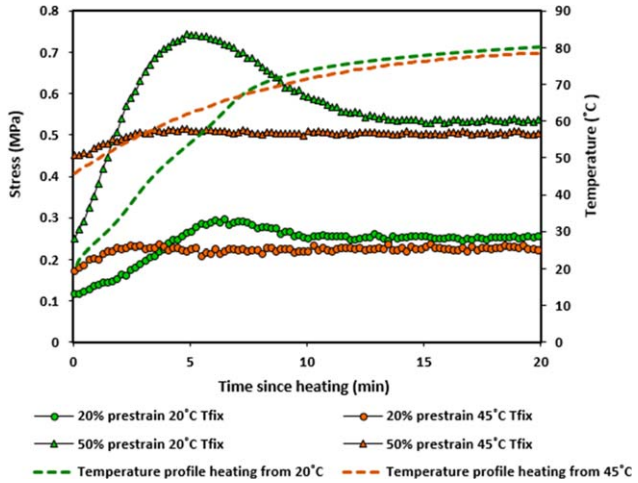

Figure 5. Experimental results from the recovery test showing stress evolution and temperature profile as a function of time. [Color figure can be viewed in the online issue, which is available at wileyonlinelibrary.com.]

memory behaviors. In other words, the stress memory phenomenon mainly occurs within a certain limit, here under the limiting stretch. Over the limiting stretch, the stress cannot be fully memorized (see the evidence of Figure 9 to be discussed later).

Programming and Stress Memory Results

The protocol of the programming and stress memory experiment was designed based on the glass transition nature of the SMP material. Since the polymer system has a glass transition zone from 43 to 78°C (Figure 4), the programming temperature is assigned to be 80°C, which provides adequate freedom for the crosslinked net-points to assist in forming the temporary shape and thus allows the stress-memory creation process (SMCP). The fixation temperatures are assigned to be 20°C (below T_g) and 45°C (within the T_g region), respectively to study the effect of T_{fix} on the recovery stress. During the recovery step, the final temperature is increased to 80°C again, which allows fully recovery of the polymer network.

The results from the constrained stress recovery test describing the stress evolution and temperature profile as a function of time are shown in Figure 5. From Figure 5, for the groups with 20°C fixation temperature, both the 20% prestrain and the 50% prestrain groups exhibit recovery stress peaks and then plateaus. However, the recovery stress peak of the 50% prestrain group (about 0.73 MPa) is much larger than that of the 20% prestrain group (about 0.29 MPa). In addition, the stabilized stress level of the 50% prestrain group (about 0.53 MPa) is also higher than that of the 20% prestrain group (about 0.25 MPa). This could be caused by the residual programming stress level. For instance, the stabilized residual stress level after programming for the 50% prestrain group is higher than that for the 20% prestrain group. Since there is no unloading during the thermo-mechanical experiment, the residual stress subsequently contributes to the peak and stabilized level of the recovery stress, and thus a higher value of the recovery stress for the 50% prestrain group. In addition to the residual programming stress, the strain hardening effect also plays an important role. For example, the 50% prestrain leads to higher modulus, thus higher

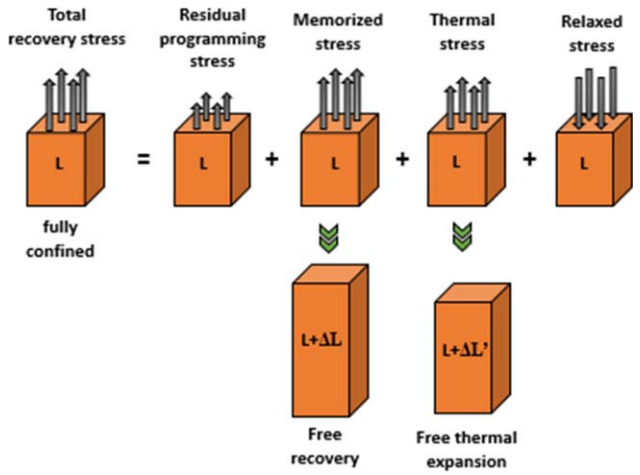

Figure 6. A schematic representation of the decomposition for the recovery stress of compression programmed SMP. [Color figure can be viewed in the online issue, which is available at wileyonlinelibrary.com.]

recovery stress. Moreover, with the temperature profile unchanged, the time it takes to reach the recovery stress peak for the 50% prestrain group is about 5 min, which is less than that for the 20% prestrain group, which is about 7 min. The recovery speed is related to the entropy increasing rate within the material.[57] It indicates that the entropy increasing rate of the 50% prestrain group is faster than that of the 20% prestrain group during the recovery, which could be attributed to a higher entropic force due to a higher prestrain level.

For the groups with 45°C fixation temperature, neither the 20% prestrain nor the 50% prestrain group shows substantial recovery effect. This is not surprising since the fixation temperature of 45°C falls within the glass transition zone, resulting in a poor stored energy during the fixation, and thus a poor output of the recovery stress during the recovery process. The purpose of conducting the experiments with 45°C T_{fix} is to verify our phenomenological model to be discussed in the next section.

Formulation of Recovery Stress

In this study, we propose that the overall recovery stress is a result of four components, including (1) residual programming stress, (2) memorized stress, (3) thermal stress, and (4) relaxed stress, as demonstrated in Figure 6.

(1) The residual programming stress exists due to the particular programming process used in this study. If there is an unloading step during programming, this stress component is equal to zero. (2) During the stress recovery process, temperature rising causes shape recovery of the specimen (expansion for compression programming and shrinkage for stretch programming). Because of the fully constrained boundary condition; however, free shape recovery is not allowed, resulting in releasing the memorized stress. As shown in Figure 6, the memorized stress can be perceived as produced by firstly allowing free shape recovery of the specimen, and then pushing the specimen back to its constrained length. The stress produced by the external pushing load is equal to the memorized stress. In addition, the memorized stress is released primarily in the glass transition region, which is unique for SMPs. In other words, for this chemical crosslinked thermoset SMP, the stress memory effect in a fully confined condition is related to the shape memory effect in constraint-free condition, which is caused by the transition of a crosslinking polymer network from a state dominated by internal energy (glassy state) to a state dominated by conformational entropy (rubbery state). (3) During the stress recovery process, temperature rising causes thermal expansion of the specimen. Similarly, due to the fully constrained boundary condition, free expansion is not allowed, resulting in thermal stress. Depending on the programming type, the thermal stress may reduce (for stretch programming), or increase (for compression programming) the recovery stress. (4) Once the stress is introduced in the fully constrained specimen, stress relaxation occurs because the constrained recovery test is the configuration for the stress relaxation test. Stress relaxation reduces the recovery stress recorded in the testing machine; therefore, the recovery stress can be mathematically represented by:

$$\sigma_r = \sigma_{\text{residual}} + \sigma_{\text{memorized}} + \sigma_T - \sigma_{\text{relaxed}} \tag{1}$$

where σ_r is the recovery stress recorded by the testing machine; σ_{residual} is the residual stress from programming; $\sigma_{\text{memorized}}$ is the memorized stress; σ_T is the thermal stress, which may contribute positively or negatively to the total recovery stress, depending on the programming types; and σ_{relaxed} is the relaxed stress due to mechanical relaxation effect.

Next, we would like to determine each term in eq. (1). As the temperature increases, the stress due to shape memory is related to a frozen function φ_f, which represents the volume fraction of the frozen phase, the instantaneous modulus function $E(T)$ and an internal variable ε_r, which represents the recoverable part of the stored strain. According to the model by Liu *et al.*,[27] φ_f and $E(T)$ are given by the following relations:

$$\varphi_f = \varphi_f(T) \tag{2}$$

$$E(T) = \frac{1}{\frac{\varphi_f}{E_i} + \frac{1-\varphi_f}{E_e}} \tag{3}$$

where E_i and E_e are the modulus corresponding to the internal energetic deformation and the entropic deformation, respectively.

ε_r can be obtained by the free recovery experiment. Therefore, the memorized stress due to shape memory effect under constraint, $\sigma_{\text{memorized}}$, is given as follows:

$$\sigma_{\text{memorized}} = E(T) \cdot \varepsilon_r \cdot (1-\varphi_f) \tag{4}$$

Since it is under 1D fully confinement recovery, the thermal stress can be estimated by:

$$\sigma_T = \int_{T_0}^{T_r} E(T)\alpha(T)dT \tag{5}$$

where $\alpha(T)$ is the linear coefficient of thermal expansion (CTE), which can be measured by dynamic mechanical analysis (DMA),[46] or by linear variable differential transducer (LVDT).[8] T_0 is the starting temperature and T_r is the ending temperature during the stress memory experiment.

The relaxed stress contributes negatively to the total recovery stress. The stress relaxation process is related to the programming history, the current stress level and the temperature

Table I. Summary of the Equations Used in the Simulation

Overall recovery stress
$\sigma_r = \sigma_{residual} + \sigma_{memorized} + \sigma_T - \sigma_{relaxed}$
Memorized stress
$\sigma_{memorized} = E(T) \cdot \varepsilon_r \cdot (1 - \varphi_f)$
$\varphi_f = \varphi_f(T)$
$E(T) = \frac{1}{\frac{\varphi_f}{E_i} + \frac{1-\varphi_f}{E_e}}$
Thermal stress
$\sigma_T = \int_{T_0}^{T_r} E(T)\alpha(T)dT$
Relaxed stress
$\sigma_{relaxed} = \sigma_{eff}\left(1 - \sum_{i=1}^{n} \exp - \left(\frac{t}{\tau_i}\right)\right)$

profile. For the styrene-based SMP, the stress relaxation process can be fitted with a set of exponential decay functions as shown below, thus defining a set of relaxation times:[55,58]

$$\sigma_{relaxed} = \sigma_{eff}\left(1 - \sum_{i=1}^{n} \exp\left(-\frac{t}{\tau_i}\right)\right) \quad (6)$$

where σ_{eff} and τ_i are the effective relaxed stress and effective relaxation time,[59] which depend on the temperature profile and programming.

In summary, the 1D constitutive equations for stress recovery response are listed in Table I.

Modeling Results

The stress memory model was applied using the parameters in Table II to compare with experimental results from stress recovery tests. To obtain the memorized stress, free recovery tests are performed for the four groups with different programming conditions (20% prestrain level and 20°C T_{fix}, 20% prestrain level and 45°C T_{fix}, 50% prestrain level and 20°C T_{fix}, and 50% prestrain level and 45°C T_{fix}, respectively). The recoverable part of the stored strain ε_r can be obtained from free recovery test as described in a previous study.[60] To obtain the thermal stress, the linear coefficient of thermal expansion is measured according to the procedure described in the Ref. [8]. As shown in Figure 7, the glassy and rubbery linear CTE are obtained to be $\alpha_g = 1.05 \times 10^{-4\circ}C^{-1}$ and $\alpha_r = 2.17 \times 10^{-4\circ}C^{-1}$. In addition, the curve fitting results, shown in Figure 2 for the modulus as a function of temperature, were applied for the thermal stress calculation. It is possible to determine the stress relaxation parameters through a series of isothermal stress relaxation experiments via a modified Maxwelle-Weichert model,[59] or a multi-branch model.[61] However, for the stress memory test, the difficulty is that the relaxation time is not only dependent on the temperature profile, but also the historical stress state during the stress memory evolution. A more sophisticated model that can accurately capture the relaxed stress during the stress memory evolution is still under investigation. Here we simply adopt an empirical way described in eq. (6), where n is taken as 1 and the parameters are listed in Table II. For the residual stress, it can be directly obtained from the testing machine, which is also given in Table II.

Figure 8 presents the simulation results showing the recovery stress, memorized stress, thermal stress and relaxed stress compared with the experimental data from stress memory test. For the group with 20% prestrain level and 20°C T_{fix} [Figure 8(a)], it is seen that the simulation result is in good agreement with the experimental data. It captures the peak stress and also the stabilized stress during the recovery process. In addition, it clearly shows the contribution of each type of stress component to the total recovery stress: during the initial stage of heating (0–6 min), thermal stress increases and the memorized stress is gradually activated because the mobility of the polymer chains is increasing as the temperature approaches the glass transition region. On the other hand, when the stress level and temperature are increasing, the mechanical relaxation accelerates, resulting in a rise in the relaxed stress. As long as the rate of change for the contributive stress (thermal stress and memorized stress) is larger than that of the relaxed stress, i.e., $d\sigma_{memorized}/dt + d\sigma_T/dt > d\sigma_{relaxed}/dt$, the recovery stress will increase; Once the rate of change of the contributive stress equals that of the relaxed stress, i.e., $d\sigma_{memorized}/dt + d\sigma_T/dt = d\sigma_{relaxed}/dt$, the recovery stress will reach its peak. This is what happened at around 7 min since heating, and the recovery stress reaches a peak of 0.3 MPa; upon further heating to 80°C (8–20 min), the thermal stress reaches a stabilized level due to little change of temperature, and the memorized stress also gradually reaches a stabilized level due to fully release of stored energy, and yet the stress is still relaxing due to the hysteresis nature of the relaxation process,[62,63] leading to $d\sigma_{memorized}/dt + d\sigma_T/dt < d\sigma_{relaxed}/dt$, and the recovery stress decreases until, eventually, the relaxed stress reaches a stabilized level, i.e., $d\sigma_{memorized}/dt + d\sigma_T/dt = d\sigma_{relaxed}/dt$ again, and the recovery stress is stabilized at about 0.22 MPa.

Similar discussions can also be made for the other three groups [Figure 8(b–d)]. This model can clearly demonstrate the fact that if the fixation temperature is located within the glass transition zone, regardless of the prestrain levels, there will be little recovery stress [Figure 8(b,d)]. In addition, the selection of the relaxation parameters listed in Table II is reasonable. For example, with the same prestrain level, a higher starting temperature during heating leads to a shorter relaxation time, i.e., with 20% prestrain, the group heating from 45°C has a τ_{eff} of 3.18 min, which is less than that of the group heating from 20°C (3.85 min). With 50% prestrain, the group heating from 45°C

Table II. Parameters Used in the Simulation for the Stress Recovery

Parameter	Value	Description
T_g (°C)	43	Onset of glass transition
α (°C^{-1})	1.05×10^{-4} (at glassy state)	Linear coefficient of thermal expansion
	2.17×10^{-4} (at rubbery state)	
E (MPa)	124 (at glassy state)	Compressive stiffness
	1.15 (at rubbery state)	
T_o (°C)	20 (20% prestrain level and 20°C T_{fix})	Starting temperature of the stress memory experiment
	45 (20% prestrain level and 45°C T_{fix})	
	20 (50% prestrain level and 20°C T_{fix})	
	45 (50% prestrain level and 45°C T_{fix})	
T_r (°C)	80 for all the groups	Ending temperature of the stress memory experiment
ε_r	0.19 (±0.01) (20% prestrain level and 20°C T_{fix})	Recoverable part of the stored strain
	0.16 (±0.01) (20% prestrain level and 45°C T_{fix})	
	0.38 (±0.03) (50% prestrain level and 20°C T_{fix})	
	0.36 (±0.03) (50% prestrain level and 45°C T_{fix})	
σ_{eff} (MPa)	0.44 (20% prestrain level and 20°C T_{fix})	Effective relaxed stress
	0.20 (20% prestrain level and 45°C T_{fix})	
	0.49 (50% prestrain level and 20°C T_{fix})	
	0.42 (50% prestrain level and 45°C T_{fix})	
τ_{eff} (min)	3.85 (20% prestrain level and 20°C T_{fix})	Effective relaxation time
	3.18 (20% prestrain level and 45°C T_{fix})	
	3.76 (50% prestrain level and 20°C T_{fix})	
	2.94 (50% prestrain level and 45°C T_{fix})	
$\sigma_{residual}$ (MPa)	0.11 (±0.02) (20% prestrain level and 20°C T_{fix})	Residual programming stress
	0.16 (±0.02) (20% prestrain level and 45°C T_{fix})	
	0.24 (±0.03) (50% prestrain level and 20°C T_{fix})	
	0.44 (±0.04) (50% prestrain level and 45°C T_{fix})	

has a τ_{eff} of 2.94 min, which is less than that of the group heating from 20°C (3.76 min).

For the group with 50% programming strain and 20°C T_{fix} [Figure 8(c)], it is seen that the peak of the recovery stress from experiment (0.74 MPa), is higher than that from simulation (0.6 MPa). One reason from macroscopic viewpoints could be that the large prestrain of 50% introduces considerable strain-hardening effect, as illustrated in Figure 3. For example, at 80°C, the rubbery modulus for the 20% prestrain sample is about 1.1MPa, whereas it increases to 1.4 MPa for the 50% prestrain sample. In other words, the modulus as a function of temperature may vary in the 50% large prestrain case. Consequently, the memorized stress and thermal stress may also vary, and so does the recovery stress. Another explanation from microscopic viewpoints could be that the strain hardening effect would lead to internal macromolecular rearrangement, thus a change of the entropy increasing rate and consequently affect the recovery speed. From Figure 8(c), the recovery stress from experiment reaches its peak a little earlier than that of simulation, indicating a faster entropy increasing rate due to the hardening effect. It is recommended that the nonlinear relaxation effect be considered, for instance, introducing the nonexponential Kohlrausch–Williams–Watts (KWW) equation,[55] to more accurately describe the stress relaxation. It is also recommended that the temperature effect on structural relaxation, thus stress relaxation be considered, such as introducing a shifting factor,[64,65] or a "reduced time."[61]

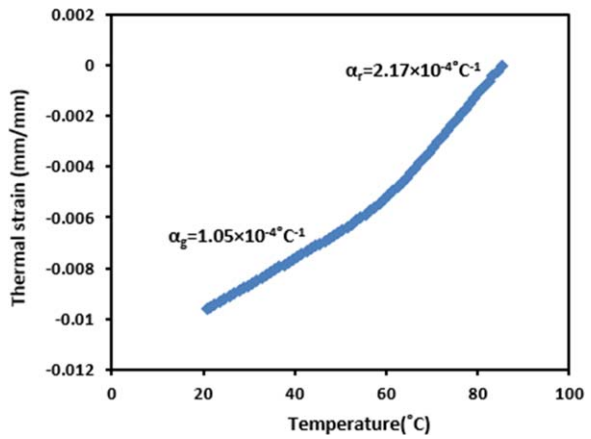

Figure 7. Thermal expansion response of the SMP material. [Color figure can be viewed in the online issue, which is available at wileyonlinelibrary.com.]

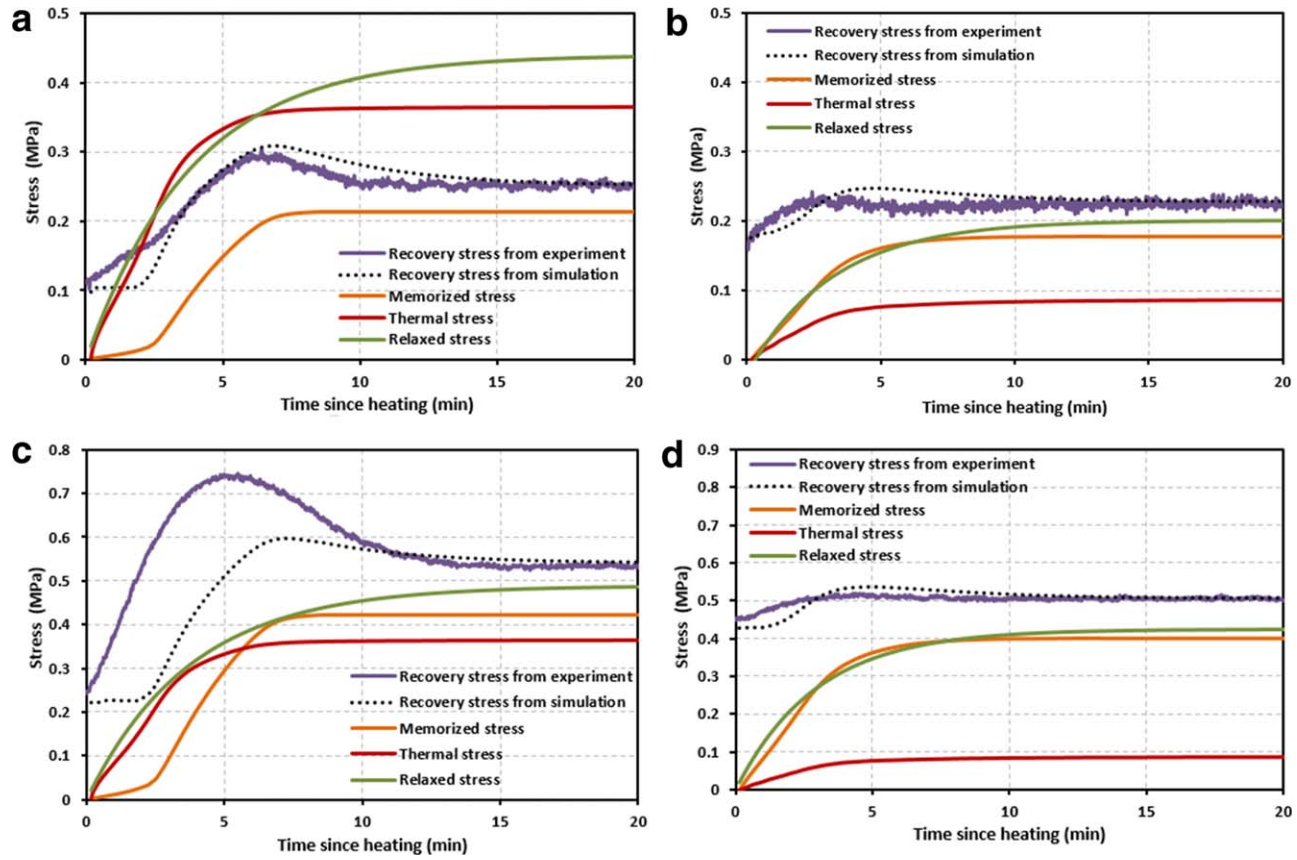

Figure 8. Simulation results showing recovery stress, memorized stress, thermal stress, and relaxed stress compared with experimental results of (a) 20% prestrain level and 20°C T_{fix}, (b) 20% prestrain level and 45°C T_{fix}, (c) 50% prestrain level and 20°C T_{fix}, and (d) 50% prestrain level and 45°C T_{fix}. [Color figure can be viewed in the online issue, which is available at wileyonlinelibrary.com.]

Since the constrained recovery test is the same configuration as the stress relaxation test, as demonstrated by Figure 1, i.e., the path (i)-(ii)-(iii)-(iv) is equivalent to path (i)-(ii)-(iii′)-(iv′). During the recovery, if without confinement, the SMP sample would expand due to shape memory and thermal expansion (step iii′), yet the sample is forced to not be expanded by an "equivalent compressive force" (step iv′). According to Newton's law, the "equivalent compressive force" must be equal to the total recovery force at the stabilized stage in order to maintain static equilibrium. For the 20% programmed strain level and 20°C T_{fix} group, the "equivalent compressive stress" is about 0.21 MPa (0.19 (free recovery strain) × 1.1 (modulus at 80°C) MPa), which is close to the stabilized recovery stress of 0.24 MPa. The slight difference is believed due to the change of cross-sectional area of the specimen because of axial thermal expansion and Poisson's ratio effects during the experiment. Likewise, For the 20% programmed strain level and 45°C T_{fix} group, the "equivalent compressive stress" is about 0.18 MPa (0.16 × 1.1 MPa), which is close to the stabilized recovery stress of 0.22 MPa. For the 50% programmed strain level and 20°C T_{fix} group, the "equivalent compressive stress" is about 0.53 MPa (0.38 × 1.4 MPa), which is quite close to the stabilized recovery stress of 0.54 MPa. For the 50% programmed strain level and 45°C T_{fix} group, the "equivalent compressive stress" is about 0.50 MPa (0.36 × 1.4 MPa), which is quite close to the stabilized recovery stress of 0.51 MPa. In others words, the proposed model works well as supported by experimental evidence shown in Figure 5.

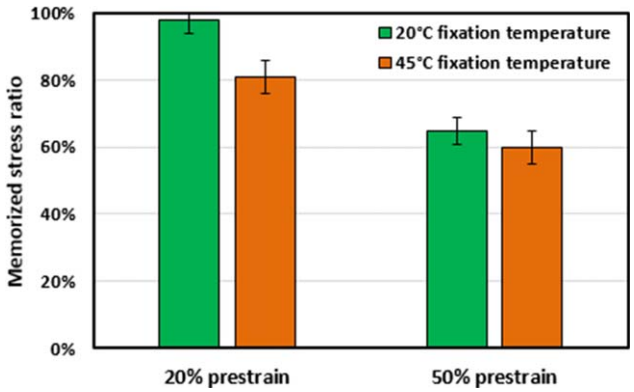

Figure 9. The memorized stress ratio for the 20% prestrain and 20°C T_{fix}, 20% prestrain and 45°C T_{fix}, 50% prestrain and 20°C T_{fix}, and 50% prestrain and 45°C $T_{fix,}$ respectively. [Color figure can be viewed in the online issue, which is available at wileyonlinelibrary.com.]

Rather than fitting one or two sets of test data, the aim of this study is to interpret the general stress recovery behaviors, such as "stress plateau," "stress undershoot," and "stress overshoot." According to our model, the total recovery stress can be

Table III. A Comparison Between Memorized Stress Ratio and Recovery Stress Ratio

	20% prestrain and 20°C T^{fix} (%)	20% prestrain and 45°C T^{fix} (%)	50% prestrain and 20°C T^{fix} (%)	50% prestrain and 45°C T^{fix} (%)
R^{memory}	98 (±3)	81 (±4)	65 (±3)	60 (±4)
$R^{recovery}$	116 (±5)	103 (±6)	81 (±6)	77 (±5)

decomposed into two parts, the contributive part and the impeditive part. For compression programming, the contributive part includes the memorized stress and thermal stress; and the impeditive part consists of the relaxed stress. For stretch programming, the contributive part of stress is the memorized stress and the impeditive part of stress includes the thermal stress and relaxed stress. Therefore, the "stress plateau" case can be explained as that the rate of stress increase due to the contributive part is equal to the rate of stress reduction due to the impeditive part, i.e., as the recovery stress approaches to a plateau, $d\sigma_{contributive}/dt = d\sigma_{impeditive}/dt$. In the "stress overshoot" case, initially the recovery stress is rising towards a peak, and thus $d\sigma_{contributive}/dt > d\sigma_{impeditive}/dt$; at the overshoot peak, $d\sigma_{contributive}/dt = d\sigma_{impeditive}/dt$; and then the recovery stress drops from the peak and $d\sigma_{contributive}/dt < d\sigma_{impeditive}/dt$. Similarly, in the "stress undershoot" case, initially $d\sigma_{contributive}/dt < d\sigma_{impeditive}/dt$, when recovery stress is dropping; at the undershoot peak, $d\sigma_{contributive}/dt = d\sigma_{impeditive}/dt$; and then recovery stress increases and $d\sigma_{contributive}/dt > d\sigma_{impeditive}/dt$.

This model may provide some guidance for polymer engineers when design of high performance SMPs for stress recovery applications. For instance, to obtain a stable and higher recovery stress one should design a polymer system that can maximize the memorized stress, increase the thermal stress (for compression programming) or decrease the thermal stress (for stretch programming) by all means, and minimize the relaxed stress, such as introducing SMP composites/nanocomposites, etc.

Memorized Stress Ratio versus Recovery Stress Ratio

To evaluate the stress memory performance, the memorized stress ratio is computed for each group, which is defined as follows,

$$R_{memory} = \frac{\sigma_{memory}}{\sigma_{programming}} \times 100\% \quad (7)$$

where R_{memory} is the memorized stress ratio, σ_{memory} is the stabilized memorized stress, and $\sigma_{programming}$ is the peak stress during programming.

On the other hand, the recovery stress ratio is defined as:

$$R_{recovery} = \frac{\sigma_r}{\sigma_{programming}} \times 100\% \quad (8)$$

where $R_{recovery}$ is the recovery stress ratio, σ_r is the stabilized value of the recovery stress.

The memorized stress ratio evaluates the stress memory performance, which is closely related to the shape memory mechanism, whereas the recovery stress ratio reflects the recovery performance of the total stress which implicitly involves all the four type of stress components (i.e., residual programming stress, memorized stress, thermal stress, and relaxed stress). Table III clearly shows the distinctive quantitative difference between the memorized stress ratio and the recovery stress ratio for each group. It is seen that the recovery stress ratio is higher than the memorized stress ratio. Intriguingly, for some groups, the recovery stress ratio is greater than 100%, i.e., the total recovery stress is even greater than the stress during programming. Take the 20% prestrain programming and 20°C fixation temperature group as an example, the recovery stress ratio $R_{recovery}$ is 116%, indicating that the stabilized recovery stress level is 16% higher than the peak stress level during programming. It is true that the modulus of the sample may be a key factor for the recovery stress, but note that both the peak programming stress and stabilized recovery stress are recorded at the rubbery state with comparable rubbery modulus. In fact, some other researchers also observed a similar effect called "stress overshoot," and attributed it to a combined effect of the variations in the viscous strain rate and viscosity under structural relaxation and mechanical relaxation during constrained recovery.[31,46] Here, we believe that there are competing stresses during the constrained stress recovery test. On one hand, release of the memorized stress and accumulation of the thermal stress lead to stress increase; on the other hand, stress relaxation (constrained stress recovery test is also a configuration for stress relaxation test) leads to stress reduction. The stress becomes maximum (overshoot) when the rate of stress increases is equal to the rate of stress reduction. After the overshoot point, the rate of stress relaxation is greater than the rate of stress increases, leading to gradual stress reduction, and finally the stress stabilizes at a level equal to or lower than the programming stress. It is also noted that the memorized stress ratio R_{memory} is consistently less than 100%, i.e., smaller than the programming stress, which is expected. Obviously, memorized stress ratio yields a more conservative reasonable result, which is important for design of SMP devices.

As shown in Figure 9, the 20% prestrain group has a higher memorized stress ratio than the 50% prestrain group, for both fixation temperatures (20 and 45°C). With a presrtain of 50%, which is clearly above the limiting stretch of the polymer network (Figure 3), the SMP sample "lost" some memory about the stress. This could attribute to the loss of cohesive energy due to friction between macromolecules under a higher mechanical load.[66] The group with 20°C fixation temperature has a higher memorized stress ratio than the group with 45°C fixation temperature, for both prestrains (20% and 50%), due to a higher stored energy. In other words, a higher memorized stress ratio requires a proper set of programming conditions (here, a lower programming strain of 20% and a lower fixation temperature of 20°C). The results are consistent with some of the previous findings. For example, the level of deformation

strongly affects the memorized stress,[24] and lowering the temperature of prestrain fixation has a strong effect on the stress memory in constraint recovery.[29] For amorphous cross-linked SMPs, the stress memory ability strongly depends on the set of crosslinks. The covalently crosslinked amorphous networks that consists of functional monomers and crosslinking agents, enable the mechanical energy to temporarily store and subsequently release, in the form of memorized stress. Therefore, variance of programming conditions essentially affects the microstructure and thus the stress memory performance.

CONCLUSIONS

In this study, the stress recovery and memory behavior for an amorphous covalently crosslinked SMP is investigated experimentally and numerically. Results indicated that the group with 20% prestrain and 20°C fixation temperature yields a higher memorized stress ratio. The simulation result for the recovery stress basically agrees with the experimental data, except for the peak recovery stress of the 50% prestrain group, due to the strain hardening and nonlinear stress relaxation effect. On the basis of the results of the experiment and simulation, the following conclusions are obtained:

- A phenomenological model is developed which considered the recovery stress as a sum of the residual programming stress, memorized stress, thermal stress, and relaxed stress. The model helps in understanding the peculiar stress recovery behaviors, such as "stress plateau," "stress undershoot," and "stress overshoot," which is crucial for design of high performance SMPs in stress demand applications.
- Memorized stress and recovery stress ratios are two different concepts. In this study, the memorized stress ratio is consistently lower than the recovery stress ratio. The memorized stress, which is always equal to or smaller than the programming stress, and the memorized stress ratio, are better indicators than the recovered stress and recovery stress ratio in characterizing the memory capability of SMPs.
- The memorized stress for an amorphous thermosetting SMP requires a set of proper programming conditions to achieve a higher memorized stress ratio.

ACKNOWLEDGMENTS

This study is sponsored by NSF under grant number CMMI 1333997. Dr. Harper Meng helped prepare the SMP material. His assistance is greatly appreciated.

REFERENCES

1. Behl, M.; Lendlein, A. *Mater. Today* **2007**, *10*, 20.
2. Liu, C.; Qin, H.; Mather, P. T. *J. Mater. Chem.* **2007**, *17*, 1543.
3. Leng, J.; Lan, X.; Liu, Y.; Du, S. *Prog. Mater. Sci.* **2011**, *56*, 1077.
4. Xie, T. *Polymer* **2011**, *52*, 4985.
5. Hu, J.; Zhu, Y.; Huang, H.; Lu, J. *Prog. Polym. Sci.* **2012**, *37*, 1720.
6. Sun, L.; Huang, W. M.; Ding, Z.; Zhao, Y.; Wang, C. C.; Purnawali, H.; Tang, C. *Mater. Des.* **2012**, *33*, 577.
7. Meng, H.; Li, G. *Polymer* **2013**, *54*, 2199.
8. Li, G.; Xu, W. *J. Mech. Phys. Solids* **2011**, *59*, 1231.
9. Li, G.; Shojaei, A. *Proc. R. Soc. A* **2012**, *468*, 2319.
10. Ping, P.; Wang, W.; Chen, X.; Jing, X. *J. Biomacromolecules* **2005**, *6*, 587.
11. Wang, W.; Jin, Y.; Ping, P.; Chen, X.; Jing, X.; Su, Z. *Macromolecules* **2010**, *43*, 2942.
12. Lendlein, A.; Kelch, S. *Angew. Chem. Int. Ed.* **2002**, *41*, 2034.
13. Zhang, Q.; Yang, Q. S. *J. Appl. Polym. Sci.* **2012**, *123*, 1502.
14. Lendlein, A.; Langer, R. *Science* **2002**, *296*, 1673.
15. Maitland, D. J.; Metzger, M. F.; Schumann, D.; Lee, A.; Wilson, T. S. *Lasers Surg. Med.* **2002**, *30*, 1.
16. Li, G.; Nettles, D. *Polymer* **2010**, *51*, 755.
17. Li, G.; Uppu, N. *Compos. Sci. Technol.* **2010**, *70*, 1419.
18. Nji, J.; Li, G. *Polymer* **2010**, *51*, 6021.
19. Nji, J.; Li, G. *Smart Mater. Struct.* **2010**, *19*, 035007.
20. John, M.; Li, G. *Smart Mater. Struct.* **2010**, *19*, 075013.
21. Li, G.; Meng, H.; Hu, J. J. R. *Soc. Interface* **2012**, *9*, 3279.
22. Li, G.; Ajisafe, O.; Meng, H. *Polymer* **2013**, *54*, 920.
23. Li, G.; Zhang, P. *Polymer* **2013**, *54*, 5075.
24. Ivens, J.; Urbanus, M.; De Smet, C. *Express. Polym. Lett.* **2011**, *5*, 254.
25. Yang, Q.; Li, G. *J. Polym. Sci. Part B: Polym. Phys.* **2014**, *52*, 1429.
26. Tobushi, H.; Okumura, K.; Hayashi, S.; Ito, N. *Mech. Mater.* **2001**, *33*, 545.
27. Liu, Y.; Gall, K.; Dunn, M. L.; Greenberg, A. R.; Diani, J. *Int. J. Plast.* **2006**, *22*, 279.
28. Véchambre, C.; Buléon, A.; Chaunier, L.; Gauthier, C.; Lourdin, D. *Macromolecules* **2011**, *44*, 9384.
29. Arrieta, J. S.; Diani, J.; Gilormini, P. *J. Appl. Polym. Sci.* **2014**, *131*, 39813.
30. Qi, H. J.; Nguyen, T. D.; Castro, F.; Yakacki, C. M.; Shandas, R. *J. Mech. Phys. Solids* **2008**, *56*, 1730.
31. Castro, F.; Westbrook, K. K.; Long, K. N.; Shandas, R.; Qi, H. J. *Mech. Time-Depend. Mater.* **2010**, *14*, 219.
32. Azra, C.; Plummer, C. J. G.; Månson, J. A. E. *Smart Mater. Struct.* **2011**, *20*, 082002.
33. Huang, W. M.; Yang, B.; Fu, Y. Q. Polyurethane Shape Memory Polymers; CRC Press: New York, **2011**.
34. Khan, F.; Koo, J. H.; Monk, D.; Eisbrenner, E. *Polym. Test* **2008**, *27*, 498.
35. Liu, Y.; Gall, K.; Dunn, M. L.; McCluskey, P. *Smart Mater. Struct.* **2003**, *12*, 947.
36. Gall, K.; Yakacki, C. M.; Liu, Y.; Shandas, R.; Willett, N.; Anseth, K. S. *J. Biomed. Mater. Res. Part A* **2005**, *73*, 339.
37. Xu, W.; Li, G. *Int. J. Solids Struct.* **2010**, *47*, 1306.
38. Wang, Z.; Li, D.; Xiong, Z.; Chang, R. *J. Appl. Polym. Sci.* **2009**, *113*, 651.
39. Chen, Y. C.; Lagoudas, D. C. *J. Mech. Phys. Solids* **2008**, *56*, 1752.

40. Chen, Y. C.; Lagoudas, D. C. *J. Mech. Phys. Solids* **2008**, *56*, 1766.
41. Tobushi, H.; Hashimoto, T.; Hayashi, S.; Yamada, E. *J. Intell. Mater. Syst. Struct.* **1997**, *8*, 711.
42. Diani, J.; Liu, Y.; Gall, K. *Polym. Eng. Sci.* **2006**, *46*, 486.
43. Nguyen, T. D.; Qi, H. J.; Castro, F.; Long, K. N. *J. Mech. Phys. Solids* **2008**, *56*, 2792.
44. Nguyen, T.; Yakacki, C. M.; Brahmbhatt, P. D.; Chambers, M. L. *Adv. Mater.* **2010**, *22*, 3411.
45. Xu, W.; Li, G. *J. Appl. Mech. Trans. ASME* **2011**, *78*, 061017.
46. Westbrook, K. K.; Kao, P. H.; Castro, F.; Ding, Y.; Qi, H. J. *Mech. Mater.* **2011**, *43*, 853.
47. Xiao, R.; Choi, J.; Lakhera, N.; Yakacki, C. M.; Frick, C. P.; Nguyen, T. D. *J. Mech. Phys. Solids* **2013**, *61*, 1612.
48. Arrieta, S.; Diani, J.; Gilormini, P. *Mech. Mater.* **2014**, *68*, 95.
49. Chen, J.; Liu, L.; Liu, Y.; Leng, J. *Smart Mater. Struct.* **2014**, *23*, 055025.
50. Shojaei, A.; Li, G. *Proc. R. Soc. A* **2014**, *470*, 20140199.
51. Tong, T. H. WO Pat. WO/2002/059,170 **2002**.
52. Di Prima, M.; Gall, K.; McDowell, D. L.; Guldberg, R.; Lin, A.; Sanderson, T.; Campbell, D.; Arzberger, S. C. *Mech. Mater.* **2010**, *42*, 304.
53. Kim, J. W.; Medvedev, G. A.; Caruthers, J. M. *Polymer* **2013**, *54*, 3949.
54. Anthamatten, M.; Roddecha, S.; Li, J. H. *Macromolecules* **2013**, *46*, 4230.
55. Strobl, G. The Physics of Polymers: Concepts for Understanding Their Structures and Behavior; Springer: Berlin, **2007**.
56. Arruda, E. M.; Boyce, M. C. *J. Mech. Phys. Solids* **1993**, *41*, 389.
57. Yu, K.; Ge, Q.; Qi, H. J. *Polymer* **2014**, *23*, 5938.
58. Messé, L.; Pézolet, M.; Prud'homme, R. *Polymer* **2001**, *42*, 563.
59. Heuchel, M.; Cui, J.; Kratz, K.; Kosmella, H.; Lendlein, A. *Polymer* **2010**, *51*, 6212.
60. Wang, A.; Li, G.; Meng, H. *Smart Mater. Struct.* **2013**, *22*, 085033.
61. Yu, K.; Ge, Q.; Qi, H. J. *Nat. Commun.* **2014**, *5*, 3066.
62. Wang, Z.; Li, Z.; Wang, L.; Xiong, Z.; Zhengdao, W. *J. Appl. Polym. Sci.* **2010**, *118*, 1406.
63. Song, W.; Wang, Z. *J. Appl. Polym. Sci.* **2013**, *128*, 199.
64. Ge, Q.; Yu, K.; Ding, Y.; Qi, H. J. *Soft Matter* **2012**, *8*, 11098.
65. Yu, K.; McClung, A. W.; Tandon, G.; Baur, J.; Qi, H. J. *Mech. Time Depend. Mater.* **2014**, *18*, 453.
66. Farzaneh, S.; Fitoussi, J.; Lucas, A.; Bocquet, M.; Tcharkhtchi, A. *J. Appl. Polym. Sci.* **2013**, *128*, 3240.